On the Molecular/Solid-State Boundary. A Cyclic Iron-Sulfur Cluster of Nuclearity Eighteen: Synthesis, Structure, and Properties

Jing-Feng You,[†] Barry S. Snyder,[†] Georgia C. Papaefthymiou,[‡] and R. H. Holm*,[†]

Contribution from the Department of Chemistry, Harvard University, Cambridge, Massachusetts 02138, and the Francis Bitter National Magnet Laboratory, Massachusetts Institute of Technology, Cambridge, Massachusetts 02139. *Received May 30, 1989*

Abstract: The reaction system $FeCl_3$:3.15Na[PhNC(O)Me]:1.78Li_2S in ethanol/methanol (2:1 (v/v)) affords, after the addition of Pr_4NBr and a 5-day period of reaction and crystallization, the black compound $(Pr_4N)_6Na_4Fe_{18}S_{30}$ in 60–75% yield. When this material is very slowly crystallized from acetonitrile/ether, the solvated compound $(Pr_4N)_6Na_4Fe_{18}S_{30}$·14MeCN is obtained. This compound crystallizes in triclinic space group $P\bar{1}$ with a = 16.286 (8) Å, b = 16.718 (8) Å, c = 17.902 (9) Å, α = 115.28 (3)°, β = 91.07 (4)°, γ = 101.64 (4)°, and Z = 1. The structure was refined to R = 6.5%. The crystal structure consists of discrete Pr_4N^+ ions and two Na^+ ions weakly associated with the cluster $[Na_2Fe_{18}S_{30}]^{8-}$, which has a remarkable and unprecedented structure. It is constructed by the fusion of 24 nonplanar Fe_2S_2 rhombs in edge- and corner-sharing modes such that there are 20 μ_2-S, 8 μ_3-S, and 2 μ_4-S, every FeS_4 unit is tetrahedral, and the 18 Fe atoms are essentially planar. The result is a cyclic or toroidal structure, of lateral dimensions 13.3 × 16.0 Å and a maximum thickness of ca. 3.3 Å, in which there are no terminal ligands. Two Na^+ ions are bound to interior sulfur atoms of the cluster, whose framework can be considered to arise from the sequential connection of known Fe_3S_4 and Fe_6S_9 cluster cores. Alternative conceptions of cluster buildup in terms of shared Fe_2S_2 rhombs and FeS_4 tetrahedra are presented and illustrated. The cyclic cluster is isolated from reaction solutions whose absorption spectra indicate the presence of the green linear chain polymer $\{[FeS_2]^-\}_n$ (λ_{max} 435, 530, 618 nm). $[Na_2Fe_{18}S_{30}]^{8-}$ forms brown solutions (λ_{max} 396, 520 (sh), 600 (sh)). The cluster is mixed valence (14Fe(III) + 4Fe(II)), is antiferromagnetic with a singlet ground state, and from its Mössbauer spectrum does not contain localized Fe(II) sites and thus is substantially electronically delocalized. The integrity of the cyclic structure in solution is indicated by its absorption and ^{23}Na NMR spectra and the retention of the Mössbauer spectrum of the solid compound. In Me_2SO solution the cluster is unreactive to NaSPh, forms $[Fe_4S_4(S\text{-}p\text{-}tol)_4]^{2-}$ with excess *p*-toluenethiol, and affords a mixture of $[Fe_4S_4(SPh)_4]^{2-}$ (major product) and $[Fe_2S_2(SPh)_4]^{2-}$ with $[Fe(SPh)_4]^{2-}$. From calculations at the extended-Hückel level, the cluster has a quasi-band structure in which orbitals divide into at least four well-separated blocks. Certain aspects of the electronic structure are briefly considered. Cluster size and structural relationships to binary and ternary Fe–S phases place $[Na_2Fe_{18}S_{30}]^{8-}$ on the boundary of molecular and solid-state compounds.

Iron–sulfur clusters present the best expression of how a fundamental building block can be elaborated into a large family of molecules with widely different structures and properties.[1-15] The building block in question is the Fe_2S_2 rhomb **1** shown in Figure 1. It is found in the simple clusters $[Fe_2S_2L_4]^{2-}$,[1-3] which closely resemble the binuclear sites in ferredoxin proteins.[4] In its more general occurrence, rhomb **1** is dimensionally variable, being found in both planar and nonplanar conformations and having Fe–S and Fe–Fe distances that usually fall in the intervals 2.15–2.35 and 2.65–2.80 Å, respectively, with concomitant ranges of bond angles. While purely conceptual, it is highly instructive to examine the assembly of clusters from such rhombs. This matter is illustrated in Figure 1.

Cluster Buildup from Fe_2S_2 Rhombs. The sharing of an edge affords the Fe_3S_3 bis-rhomb **2** while Fe and S vertex-sharing leads to bis-rhombs Fe_3S_4 (**3**) and Fe_4S_3 (**4**), respectively. Each of these can be elaborated further by edge-sharing and/or vertex-sharing such that a resultant structure can contain some combination of the three known sulfur bridging modes, μ_2-S, μ_3-S, and μ_4-S. Without exception, the stereochemistry at these bridge atoms is bent, trigonal pyramidal, and square pyramidal or tetrahedral, respectively. These entities constitute the cluster *cores* $[Fe_xS_y]^z$ in which there are two or three, but not more, Fe–S bonds to a single Fe atom, sulfur is present as sulfide only, and terminal ligation is completed in nearly all cases by a unidentate ligand L, affording the tetrahedral unit FeS_3L. The absence of higher Fe coordination numbers within the core is presumably determined by size and charge restrictions. Terminal ligands L are RS^-, RO^-, halide, or PR_3 in practically all known Fe–S clusters of the types considered here. With these regularities in mind, cluster buildup is examined.

Creation of a third rhomb by sharing adjacent edges of bis-rhomb **2** yields the Fe_3S_4 core **5**, whose existence in several proteins has recently been demonstrated.[6] Two more steps of edge-sharing afford the Fe_4S_4 cubane core **6**, which occurs in numerous Fe–S proteins[8] and is well-known in the synthetic clusters $[Fe_4S_4$-

[†] Harvard University.
[‡] Massachusetts Institute of Technology.

(1) Berg, J. M.; Holm, R. H. In *Iron–Sulfur Proteins*; Spiro, T. G., Ed.; Wiley-Interscience: New York, 1982; Chapter 1.
(2) (a) Cleland, W. E., Jr.; Averill, B. A. *Inorg. Chem.* **1984**, *23*, 4192. (b) Strasdeit, H.; Krebs, B.; Henkel, G. *Inorg. Chim. Acta* **1984**, *89*, L11. (c) Cai, J.; Cheng, C. *Jiegou Huaxue* **1988**, *7*, 43. (d) Salifoglou, A.; Simopoulos, A.; Kostikas, A.; Dunham, R. W.; Kanatzidis, M. G.; Coucouvanis, D. *Inorg. Chem.* **1988**, *27*, 3394.
(3) (a) Saak, W.; Pohl, S. *Z. Naturforsch., B: Anorg. Chem., Org. Chem.* **1985**, *40B*, 1105. (b) Cen, W.; Liu, H. *Jiegou Huaxue* **1986**, *5*, 203.
(4) (a) Tsukihara, T.; Fukuyama, K.; Nakamura, M.; Katsube, Y.; Tanaka, N.; Kakudo, M.; Wada, K.; Hase, T.; Matsubara, H. *J. Biochem. (Tokyo)* **1981**, *90*, 1763. (b) Tsutsui, T.; Tsukihara, T.; Fukuyama, K.; Katsube, Y.; Hase, T.; Matsubara, H.; Nishikawa, Y.; Tanaka, N. *J. Biochem. (Tokyo)* **1983**, *94*, 299.
(5) Hagen, K. S.; Watson, A. D.; Holm, R. H. *J. Am. Chem. Soc.* **1983**, *105*, 3905.
(6) (a) Stout, G. H.; Turley, S.; Sieker, L. C.; Jensen, L. H. *Proc. Natl. Acad. Sci. U.S.A.* **1988**, *85*, 1020. (b) Stout, C. D. *J. Biol. Chem.* **1988**, *263*, 9256; *J. Mol. Biol.* **1989**, *205*, 545. (c) Kissinger, C. R.; Adman, E. T.; Sieker, L. C.; Jensen, L. H. *J. Am. Chem. Soc.* **1988**, *110*, 8721. (d) Kissinger, C. R.; Adman, E. T.; Sieker, L. C.; Jensen, L. H.; LeGall, J. *FEBS Lett.* **1989**, *244*, 447.
(7) (a) Johnson, R. E.; Papaefthymiou, G. C.; Frankel, R. B.; Holm, R. H. *J. Am. Chem. Soc.* **1983**, *105*, 7280. (b) Mascharak, P. K.; Hagen, K. S.; Spence, J. T.; Holm, R. H. *Inorg. Chim. Acta* **1983**, *80*, 157. (c) Cleland, W. E.; Holtman, D. A.; Sabat, M.; Ibers, J. A.; DeFotis, G. C.; Averill, B. A. *J. Am. Chem. Soc.* **1983**, *105*, 6021. (d) Hagen, K. S.; Watson, A. D.; Holm, R. H. *Inorg. Chem.* **1984**, *23*, 2984. (e) Kanatzidis, M. G.; Baenziger, N. C.; Coucouvanis, D.; Simopoulos, A.; Kostikas, A. *J. Am. Chem. Soc.* **1984**, *106*, 4500. (f) Müller, A.; Schladerbeck, N.; Bögge, H. *Chimia* **1985**, *39*, 24; *J. Chem. Soc., Chem. Commun.* **1987**, 35. (g) O'Sullivan, T.; Millar, M. *J. Am. Chem. Soc.* **1985**, *107*, 4096. (h) Ollerenshaw, T. J.; Garner, C. D.; Odell, B.; Clegg, W. *J. Chem. Soc., Dalton Trans.* **1985**, 2161. (i) Ueyama, N.; Sugawara, T.; Fuji, M.; Nakamura, A.; Yasuoka, N. *Chem. Lett.* **1985**, 175. (j) Gloux, J.; Gloux, P.; Hendriks, H.; Rius, G. *J. Am. Chem. Soc.* **1987**, *109*, 3220. (k) Carney, M. C.; Papaefthymiou, G. C.; Whitener, M. A.; Spartalian, K.; Frankel, R. B.; Holm, R. H. *Inorg. Chem.* **1988**, *27*, 346. (l) Pohl, S.; Saak, W. *Z. Naturforsch., B: Anorg. Chem., Org. Chem.* **1988**, *43B*, 457.
(8) Stout, C. D. In *Iron–Sulfur Proteins*; Spiro, T. G., Ed.; Wiley-Interscience: New York, 1982; Chapter 3.

0002-7863/90/1512-1067$02.50/0

Table I. Stereochemistry of Iron-Sulfur Clusters

formula[a]	core	structure	ref
$[Fe_2S_2L_4]^{2-}$ [b]	$[Fe_2(\mu_2\text{-}S)_2]^{2+}$	planar rhomb, D_{2h} (**1**)	1–4
$[Fe_3S_4(SR)_4]^{3-}$	$[Fe_3(\mu_2\text{-}S)(\mu_2\text{-}S)_2]^{+}$	vertex-shared bis-rhomb, D_{2d} (**3**, **14**)	5
$[Fe_3S_4(SR)_3]^{2-}$ [b]	$[Fe_3(\mu_3\text{-}S)(\mu_2\text{-}S)_2]^{+}$	Fe-voided cubane, C_{3v} (**5**)	6
$[Fe_4S_4L_4]^{1-,2-,3-}$ [b]	$[Fe_4(\mu_3\text{-}S)_4]^{3+,2+,1+}$	cubane, T_d (**6**)	1, 3, 7, 8
$[Fe_4S_3(NO)_7]^{-}$	$[Fe_4(\mu_3\text{-}S)_3]^{-}$	S-voided cubane, C_{3v}	9
$[Fe_6S_6L_6]^{2-,3-}$	$[Fe_6(\mu_3\text{-}S)_6]^{3+,2+}$	prismane, D_{3h}	10
$Fe_6S_6(PR_3)_4L_2$	$[Fe_6(\mu_4\text{-}S)(\mu_3\text{-}S)_4(\mu_2\text{-}S)]^{2+}$	basket, C_{2v}	11
$[Fe_6S_8(PR_3)_6]^{2+,1+}$	$[Fe_6(\mu_3\text{-}S)_8]^{2+,1+}$	stellated octahedron,[c] O_h	12
$[Fe_6S_9L_2]^{4-}$	$[Fe_6(\mu_4\text{-}S)(\mu_3\text{-}S)_2(\mu_2\text{-}S)_6]^{2-}$	C_{2v} (**13**, **15**)	5, 13
$Fe_7S_6(PR_3)_4Cl_3$	$[Fe_7(\mu_3\text{-}S)_6]^{3+}$	monocapped prismane, C_{3v}	14
$[Fe_8S_6L_8]^{3-}$	$[Fe_8(\mu_4\text{-}S)_6]^{5+}$	stellated octahedron,[c] O_h	15
$[Na_2Fe_{18}S_{30}]^{8-}$	$[Fe_{18}(\mu_4\text{-}S)_2(\mu_3\text{-}S)_8(\mu_2\text{-}S)_{20}]^{10-}$	toroid, C_{2h}	*d*

[a] L = RS^-, RO^-, halide. [b] Biological cluster. [c] Alternatively, bicapped prismane. [d] This work.

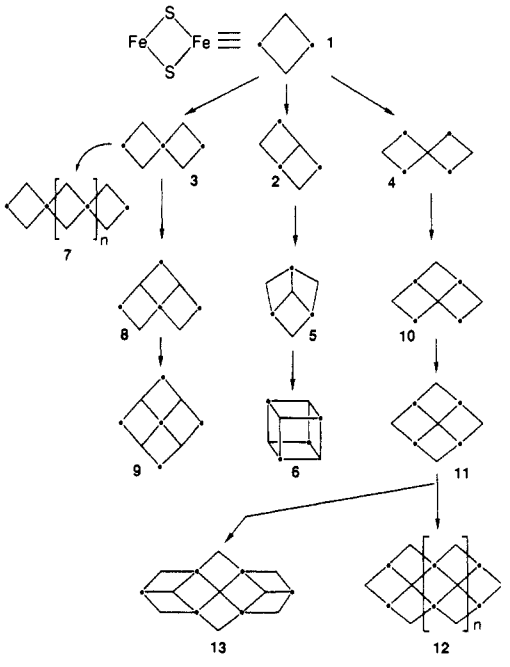

Figure 1. Schematic representation of the buildup of core units of clusters by connection of Fe_2S_2 rhombs **1** by edge-sharing (**2**), Fe vertex-sharing (**3**), and S vertex-sharing (**4**). Structures **5**–**13** are developed by additional connectivity modes of these types.

$(SR)_4]^{1-,2-,3-}$.[1,7] Cubane **6** is not readily susceptible to further buildup using the rhomb concept.[16] The stereochemistry at Fe and S is unfavorable for edge-sharing, and vertex-sharing increases coordination numbers above 4. Fusion of rhombs on opposite edges of **2** followed by two repeats and cyclization (not shown) generates the D_{3h} Fe_6S_6 core of the prismane clusters $[Fe_6S_6L_6]^{2-,3-}$.[10] Bis-rhomb **3** is the core of $[Fe_3S_4(SR)_4]^{3-}$,[5] and Fe vertex-sharing may be extended to yield, in the limit, the $^1_\infty[FeS_2]$ chains **7** in M^IFeS_2[18] and $Na_3Fe_2S_4$.[19] Adjacent edge-sharing of rhombs generates Fe_4S_4 (**8**), an unknown isomer of **6**, and Fe_5S_4 (**9**), a seemingly viable but experimentally unrealized core. Bis-rhomb **4** can be augmented by additional S vertex-sharing (not shown) and by adjacent edge-sharing to yield an Fe_4S_4 isomer (**10**) and then Fe_4S_5 (**11**), which are the inverse of **8** and **9**, respectively. The latter is a unit of some importance. It is found in the cores of the basket clusters $Fe_6S_6(PR_3)_4L_2$.[11] Further, repetition of edge-sharing generates the ribbons **12**, present in $BaFe_2S_3$,[20] and fusion of two rhombs on opposite edge pairs leads to the Fe_6S_9 core **13** of $[Fe_6S_9(SR)_2]^{4-}$.[5,13] Indeed, this core, because it integrates doubly, triply, and quadruply bridging sulfur atoms in a single structure, provides a convincing demonstration of the source of structural diversity of Fe–S clusters.

The preceding conceptual view of cluster core formation from the rhombs **1** is readily applicable to the core structures of the various types of Fe–S clusters in Table I. This compilation is limited to species in which Fe atoms are four-coordinate and includes all established modes of rhomb vertex- and edge-sharing. Structural descriptions are idealized for clarity. Structures of these cluster types are summarized elsewhere[11c] and are applicable to selenium analogues, where their structures are known. Two of these types, $[Fe_3S_4(SR)_4]^{3-}$ (**14**) and $[Fe_6S_9(SR)_2]^{4-}$ (**15**), will

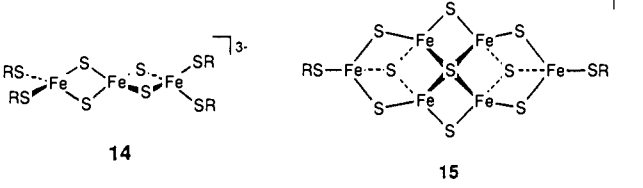

14 **15**

assume special significance in the present work. The foregoing formalism of cluster core formation immediately suggests new synthetic targets and reinforces the point that many new structures remain to be discovered. In recent experiments directed toward the synthesis of new Fe–S clusters as possible precursors to or components of the Mo/V–Fe–S cofactor of nitrogenase, we have found a reaction system that affords an entirely new type of Fe–S cluster. Its structure can be generated by the rhomb-sharing principle, but the topology departs from those of the clusters in Table I, whose nuclearities are much lower. Here we report the preparation, structure, and selected properties of $[Na_2Fe_{18}S_{30}]^{8-}$, the first cyclic cluster. The essential structural features of this cluster have been communicated recently.[21]

(9) Chu, C. T.-W.; Dahl, L. F. *Inorg. Chem.* **1977**, *16*, 3245.
(10) (a) Saak, W.; Henkel, G.; Pohl, S. *Angew. Chem., Int. Ed. Engl.* **1984**, *23*, 150. (b) Kanatzidis, M.; Hagen, W. R.; Dunham, W. R.; Lester, R. K.; Coucouvanis, D. *J. Am. Chem. Soc.* **1985**, *107*, 953. (c) Kanatzidis, M.; Salifoglou, A.; Coucouvanis, D. *Inorg. Chem.* **1986**, *25*, 2460.
(11) (a) Snyder, B. S.; Reynolds, M. S.; Noda, I. *Inorg. Chem.* **1988**, *27*, 595. (b) Snyder, B. S.; Holm, R. H. *Inorg. Chem.* **1988**, *27*, 2339. (c) Reynolds, M. S.; Holm, R. H. *Inorg. Chem.* **1988**, *27*, 4494.
(12) (a) Agresti, A.; Bacci, M.; Cecconi, F.; Ghilardi, C. A.; Midollini, S. *Inorg. Chem.* **1985**, *24*, 689. (b) Cecconi, F.; Ghilardi, C. A.; Midollini, S.; Orlandini, A.; Zanello, P. *J. Chem. Soc., Dalton Trans.* **1987**, 831.
(13) (a) Christou, G.; Sabat, M.; Ibers, J. A.; Holm, R. H. *Inorg. Chem.* **1982**, *21*, 3518. (b) Strasdeit, H.; Krebs, B.; Henkel, G. *Inorg. Chem.* **1984**, *23*, 1816. (c) Strasdeit, H.; Krebs, B.; Henkel, G. *Z. Naturforsch., B: Anorg. Chem., Org. Chem.* **1987**, *24B*, 565.
(14) Noda, I.; Snyder, B. S.; Holm, R. H. *Inorg. Chem.* **1986**, *25*, 3851.
(15) Pohl, K.; Saak, W. *Angew. Chem., Int. Ed. Engl.* **1984**, *23*, 907.
(16) Clusters of the type $[Cp_4Fe_4S_{5,6}]^{z}$ [17] might appear to be inconsistent with this treatment. However, they contain the $Fe_4(\mu_3\text{-}S)_3(\mu_3\text{-}S_2)_{1,2}$ cores with one or two $Fe(S_2)$ fragments that form a three-membered ring, not a rhomb. These and other clusters containing persulfide are beyond the purview of this description of cluster formation.
(17) (a) Vergamini, P. J.; Kubas, G. J. *Prog. Inorg. Chem.* **1976**, *21*, 261. (b) Kubas, G. J.; Vergamini, P. J. *Inorg. Chem.* **1981**, *20*, 2667. (c) Dupre, N.; Hendriks, H. M. J.; Jordanov, J.; Gaillard, J.; Auric, P. *Organometallics* **1984**, *3*, 800. (d) Dupre, N.; Auric, P.; Hendriks, H. M. J.; Jordanov, J. *Inorg. Chem.* **1986**, *25*, 1391.
(18) (a) Boon, J. W.; MacGillavry, C. H. *Recl. Trav. Chim. Pays-Bas* **1942**, *61*, 910. (b) Bronger, W. *Z. Anorg. Allg. Chem.* **1968**, *359*, 225.
(19) Klepp, K. O.; Boller, H. *Monatsh. Chem.* **1981**, *112*, 83.
(20) (a) Hong, H. Y.; Steinfink, H. *J. Solid State Chem.* **1972**, *5*, 93. (b) Steinfink, H.; Hong, H.; Grey, I. *Natl. Bur. Stand. Spec. Publ. 364*, **1972**, 681.

Table II. Crystallographic Data for $(n\text{-}Pr_4N)_6Na_4Fe_{18}S_{30}\cdot 14MeCN$

formula	$C_{100}H_{210}Fe_{18}N_{20}Na_6S_{30}$	V, Å^3	4287 (3)
mol wt	3751.90	Z	1
a, Å	16.286 (8)	space group	$P\bar{1}$
b, Å	16.718 (8)	d_{calcd},[a] g/cm^3	1.45
c, Å	17.902 (9)	μ, cm^{-1}	18.8
α, deg	115.28 (3)	$R(F_o)$, %	6.47
β, deg	91.07 (4)	$R_w(F_o^2)$, %	8.30
γ, deg	101.64 (4)		

[a] Accurate density could not be determined because of solvate composition.

Experimental Section

Preparation of Compounds. All manipulations were carried out under a pure dinitrogen/helium atmosphere. Solvents were thoroughly dried and degassed prior to use.

$(n\text{-}Pr_4N)_6Na_4Fe_{18}S_{30}$. To a vigorously stirred solution of 8.76 g (54.0 mmol) of anhydrous $FeCl_3$ in 300 mL of ethanol was added slowly a solution of 170 mmol of Na[PhNC(O)Me] in 350 mL of ethanol (prepared in situ from the reaction of equimolar quantities of acetanilide and sodium metal at 5 °C). The reaction mixture, consisting of a yellow solution and a yellow solid, was stirred for 1 h. A slurry of 4.41 g (96.0 mmol) of Li_2S in 350 mL of methanol was added dropwise with stirring over a period of 2 h until the reaction mixture just started turning dark green. At this point, about 60% of the Li_2S slurry had been added. The remaining portion of the slurry was added periodically with stirring over 10 h. The mixture was stirred for an additional 1 h and filtered. A solution of 14.4 g (54.0 mmol) of $(n\text{-}Pr_4N)Br$ in 50 mL of ethanol was added to the dark brown-green filtrate. Over a period of 5 days, the solution assumed a more nearly brown color and a dark crystalline solid separated. This material was collected by filtration, washed thoroughly with ethanol and ether, and dried in vacuo. A second crop was obtained by slowly concentrating the filtrate to half its original volume. The two crops were combined and recrystallized from acetonitrile/ether. The solid was dissolved at room temperature, the solution was filtered, and the filtrate was maintained at 5 °C for periods up to 1 week. The product slowly crystallized and was obtained as black crystals that were very easily desolvated. An X-ray structural determination showed that the crystals have the title composition and also contain 14 acetonitrile solvate molecules. The crystalline solid was washed with acetonitrile/ether (1:10 (v/v)) and ether and dried in vacuo to afford 6.9 g of product in the fully desolvated form. Yields in multiple preparations were 60–75% based on Fe. Anal. Calcd for $C_{72}H_{168}N_6Na_4S_{30}$: C, 27.22; H, 5.33; Fe, 31.64; N, 2.65; Na, 2.89; S, 30.27. Found: C, 27.20; H, 5.41; Fe, 31.40; N, 2.70; Na, 3.73; S, 29.36. High sodium analyses were obtained on other preparations as well and are presumably due to NaCl impurity. λ_{max} (ϵ_M) (acetonitrile): 300 (81 100), 320 (sh), 396 (76 400), 520 (sh), 600 (sh, 32 700).

$(n\text{-}Bu_4N)_6Na_4Fe_{18}S_{30}$. Use of the foregoing procedure with 4.41 g of Li_2S in 350 mL of ethanol and 54 mmol of $(n\text{-}Bu_4N)Br$ afforded the desolvated product as a black crystalline solid in 70–75% yield. Its absorption spectrum is identical with that of the $n\text{-}Pr_4N^+$ salt.

The compounds $(R_4N)_6Na_4Fe_{18}S_{30}$ (R = *n*-Pr, *n*-Bu) are soluble in dipolar aprotic solvents such as acetonitrile, DMF, and Me_2SO, slightly soluble in methanol where they are marginally stable but decompose at 50 °C, and considerably more soluble and stable in Na[PhNC(O)Me]/MeOH solutions. In all these media they form brown solutions. The compounds are also stable in acetonitrile up to 75 °C for at least 1 h.

Collection and Reduction of X-ray Data. Diffraction-quality crystals proved to be difficult and tedious to obtain. Very slow diffusion of ether into an acetonitrile solution of the $n\text{-}Pr_4N^+$ salt maintained to 5 °C for a period up to several months afforded well-formed black crystals. After removal from the mother liquor, they were coated with Apiezon grease. These crystals differed in their diffraction quality. A crystal was identified which, from axial photographs and peak profiles, gave evidence of a small daughter crystal with diffraction intensities <10% of the parent. No purely single crystal was obtained. Data collection was carried out at ambient temperature on a Nicolet P3F diffractometer equipped with a graphite monochromator. Unit cell parameters were obtained from 25 machine-centered reflections ($25 \le 2\theta \le 28°$). Intensities of three check reflections monitored every 123 reflections revealed a decay of ca. 15% over the course of data collection, which was corrected by processing the data sets with the program XTAPE of the SHELXTL program package (Nicolet XRD Corp., Madison, WI). An empirical absorption correction was applied with use of the program PSICOR. Simple E statistics indicated a centrosymmetric space group, $P\bar{1}$. Successful solution and refinement of the structure corroborated this choice of space group. Crystallographic data are contained in Table II.

Structure Solution and Refinement. Atom scattering factors were taken from a standard source.[22] All iron and sulfur atoms were located by direct methods using MULTAN. All carbon atoms were located in successive difference Fourier maps and were refined using CRYSTALS. Isotropic refinement converged at $R = 11.0\%$. All non-hydrogen atoms were refined anisotropically, and hydrogen atoms were included at 0.95 Å from the bonded carbon atoms and with the isotropic thermal parameter 8.0 Å^2 in the final stage of refinement. A final difference Fourier map revealed several peaks in the range 0.3–0.5 e/Å^3 that were within bonding range of the Fe atoms and are probable artifacts from crystal twinning. The small standard deviations on the positional parameters of iron and sulfur atoms indicated that the heavy-atom portion of the structure is well defined.[23]

Other Physical Measurements. All measurements were carried out under strictly anaerobic conditions. Magnetic susceptibility and Mössbauer spectroscopic measurements were performed as described elsewhere,[7k] as were absorption spectral, ^1H NMR, and electrochemical determinations.[11b] Isomer shifts of ^{57}Fe are reported relative to Fe metal at 4.2 K. Electrochemical experiments were carried out in DMF solution with a Pt working electrode, a SCE reference electrode, and 0.2 M $(n\text{-}Bu_4N)BF_4$ supporting electrolyte. ^{23}Na NMR spectra were determined at 79.4 MHz with use of a Bruker WM spectrometer; the external reference was a 0.25 M NaCl solution.

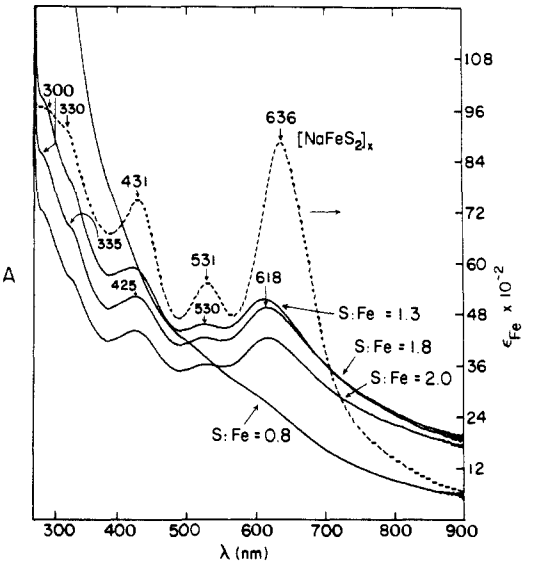

Figure 2. UV/visible absorption spectra of reaction mixtures initially containing the mole ratios $FeCl_3/3Na[PhC(O)NMe]/nLi_2S$ with $n = 0.8$ (5 h), 1.3 (18 h), 1.8 (22 h), and 2.0 (26 h) in 2:1 (v/v) ethanol/methanol measured at the indicated times after mixing. Also shown is the spectrum of polymeric $NaFeS_2$ prepared from $FeCl_3$ + 3NaSH in water at pH 12. Absorption maxima are indicated. Spectra of reaction mixtures were measured on solutions containing suspensions of small amounts of finely divided solid.

Results and Discussion

Cluster Synthesis. We have recently shown that in the self-assembly of Fe–S clusters from simple reactants, the nature of (potential) terminal ligands can alter the course of the assembly reaction. One example of this effect is the basket clusters $Fe_6S_6(PR_3)_4L_2$[11] (Table I) whose core, a topological isomer of the prismane cluster core, has not yet been formed in the absence of a tertiary phosphine. In exploring the potential of the amidate ligand $[ArNC(O)R']^-$ in this connection, we have prepared the cluster $[Na_2Fe_{18}S_{30}]^{8-}$, with an unprecedented cyclic structure. After considerable experimentation, a successful reaction system initially containing the mole ratio $FeCl_3$:3Na[PhNC(O)Me]:nLi_2S in 2:1 (v/v) EtOH/MeOH was devised.

(21) You, J.-F.; Snyder, B. S.; Holm, R. H. *J. Am. Chem. Soc.* **1988**, *110*, 6589.

(22) Cromer, D. T.; Waber, J. T. *International Tables for X-Ray Crystallography*; Kynoch Press: Birmingham, England, 1974.

(23) See the paragraph at the end of this article concerning supplementary material.

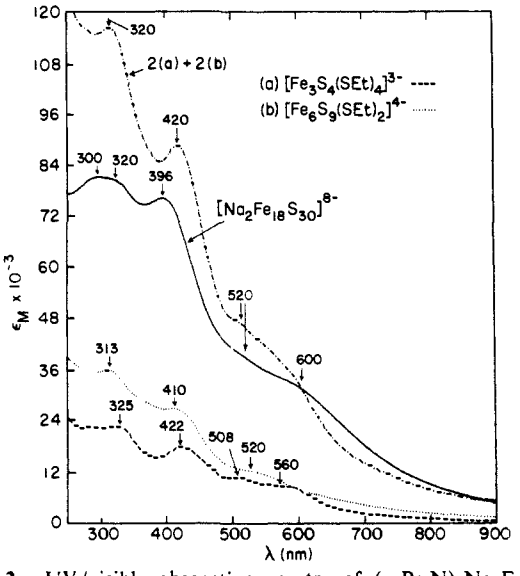

Figure 3. UV/visible absorption spectra of $(n\text{-}Pr_4N)_6Na_4Fe_{18}S_{30}$, $(Et_4N)_3[Fe_3S_4(SEt)_4]$ (a), and $(Et_4N)_4[Fe_6S_9(SEt)_2]$ (b) in acetonitrile solutions. Also shown is the calculated spectrum of 2(a) + 2(b). Absorption maxima are indicated.

The effect of varying equivalents n of sulfide reagent is shown by the UV/visible spectra in Figure 2. When n = 0.8, a brown solution is formed and a broad, featureless spectrum appears whose origin is unknown. When n = 1.3 and 1.8, the solutions are brown-green to green and their spectra have principal bands at 425, 530, and 618 nm. At n = 2.0, the solution is green with the same spectrum. This spectrum is convincingly similar to the three-band pattern (431, 531, 636 nm) observed in an alkaline colloidal solution of $NaFeS_2$[24] and also shown in Figure 2. The dark green chromophore is the polymeric anion $[FeS_2]_x^{x-}$ whose formulation **7** is based on the $^1_\infty[FeS_2]$ chains present in the solid

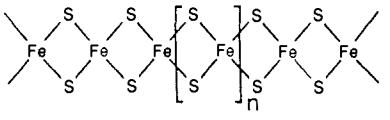

7

state.[18] From the reaction mixture, the $(n\text{-}Pr_4N)_6Na_2$ salt of $[Na_2Fe_{18}S_{30}]^{8-}$ can be obtained in 60–75% yield. The cluster is brown and its absorption spectrum, shown in Figure 3, lacks the intense visible featurs of **7**. As reported earlier,[21] a reaction mixture in methanol containing 1.3 equiv of Li_2S affords this compound in 35% yield. The analogous $n\text{-}Bu_4N^+$ salt has been isolated in 70–75% yield from a reaction mixture in ethanol containing 1.8 equiv of Li_2S. In all these mixtures, the color before cation addition has a decidedly green component. On the basis of the extinction coefficients in Figures 2 and 3, the spectrum of **7** could mask that of $[Na_2Fe_{18}S_{30}]^{8-}$, particularly above 400 nm. The yields of cluster suggest a chain → ring conversion, which is consistent with the rather slow separation of cluster salt and the gradual assumption of a nearly brown color by the solution from which the salt separates. The choice of cation is important in order to avoid precipitation of a salt of the chain anion. The sulfide:Fe(III) ratio of 1.8 is employed in order to allow partial reduction to Fe(II), whose presence is indicated by the mean oxidation state $Fe^{2.78+}$ in the product. If sulfide is oxidized to sulfur, the required exact reactant ratio is 1.78.

The role of the acetanilide anion in cluster assembly is not yet understood. If Na[PhNC(O)Me] is replaced by NaOMe in the foregoing reaction mixtures, an intractable black solid and a colorless supernatant are obtained. We speculate that the acetanilide anion has the role of kinetically suppressing linear polymer formation by acting as an end group which, however, is sufficiently labile to be displaced by sulfide in ring formation. The inclusion of two sodium ions in the cluster structure (vide infra) has the effect of partial neutralization of the high negative charge of the $Fe_{18}S_{30}$ ring.

(24) Taylor, P.; Shoesmith, D. W. *Can. J. Chem.* **1978**, *56*, 2797.

Table III. Selected Interatomic Distances (Å) for $[Na_2Fe_{18}S_{30}]^{8-}$

		Fe···Fe	
Fe(1)–Fe(2)	2.717 (3)	Fe(3)–Fe(5)	2.702 (3)
Fe(1)–Fe(9′)	2.703 (3)	Fe(6)–Fe(8)	2.672 (3)
Fe(2)–Fe(3)	2.722 (3)	Fe(4)–Fe(5)	2.783 (3)
Fe(8)–Fe(9)	2.724 (3)	Fe(6)–Fe(7)	2.738 (3)
Fe(3)–Fe(4)	2.725 (3)	Fe(4)–Fe(7)	2.771 (3)
Fe(7)–Fe(8)	2.701 (3)	Fe(5)–Fe(6)	2.761 (3)
		Fe–(μ_2-S)	
Fe(1)–S(1)	2.234 (4)	Fe(2)–S(1)	2.207 (4)
Fe(1)–S(14′)	2.235 (4)	Fe(9)–S(14)	2.210 (4)
Fe(1)–S(2)	2.267 (4)	Fe(2)–S(2)	2.227 (4)
Fe(1′)–S(15)	2.259 (5)	Fe(9)–S(15)	2.231 (5)
Fe(2)–S(4)	2.258 (4)	Fe(3)–S(4)	2.206 (4)
Fe(9)–S(13)	2.227 (4)	Fe(8)–S(13)	2.174 (4)
Fe(3)–S(6)	2.216 (4)	Fe(5)–S(6)	2.230 (4)
Fe(8)–S(12)	2.207 (4)	Fe(6)–S(12)	2.216 (4)
Fe(5)–S(7)	2.210 (4)	Fe(4)–S(9)	2.240 (4)
Fe(6)–S(7)	2.202 (4)	Fe(7)–S(9)	2.245 (4)
		Fe–(μ_3-S)	
Fe(2)–S(3)	2.361 (4)	Fe(3)–S(5)	2.293 (4)
Fe(9)–S(10)	2.385 (4)	Fe(8)–S(11)	2.265 (4)
Fe(3)–S(3)	2.296 (4)	Fe(4)–S(5)	2.303 (4)
Fe(8)–S(10)	2.310 (4)	Fe(7)–S(11)	2.273 (4)
Fe(4)–S(3)	2.287 (4)	Fe(5)–S(5)	2.318 (4)
Fe(7)–S(10)	2.287 (4)	Fe(6)–S(11)	2.299 (4)
		Fe–(μ_4-S)	
Fe(4)–S(8)	2.355 (4)	Fe(5)–S(8)	2.365 (4)
Fe(7)–S(8)	2.347 (4)	Fe(6)–S(8)	2.345 (4)
		Na···S	
Na(1)–S(2′)	2.910 (7)	Na(2)–S(2)	3.027 (8)
Na(1)–S(9)	2.871 (6)	Na(2)–S(5)	3.022 (8)
Na(1)–S(9′)	2.907 (7)	Na(2)–S(9)	3.007 (9)
Na(1)–S(10)	3.245 (7)		
Na(1)–S(15)	2.871 (7)		
		Na···N ($NCCH_3$)	
Na(1)–N(50)	2.746 (20)	Na(2)–N(50)	2.463 (18)
		Na(2)–N(60)	2.540 (21)
		Na(2)–N(70)	2.416 (28)
		S···S	
S(1)–S(2)	3.519 (5)	S(3)–S(4)	3.550 (5)
S(14)–S(15)	3.532 (6)	S(10)–S(13)	3.559 (5)
S(3)–S(5)	3.650 (5)	S(5)–S(6)	3.515 (5)
S(10)–S(11)	3.602 (5)	S(11)–S(12)	3.519 (5)
S(5)–S(8)	3.680 (5)	S(7)–S(8)	3.565 (5)
S(8)–S(11)	3.674 (5)	S(8)–S(9)	3.606 (5)
S(9)–S(9′)	4.090 (7)	S(2)–S(9)	3.986 (5)
S(1)–S(1′)	13.320	S(7)–S(7′)	15.975
		Na···Na	
Na(1)–Na(1′)	4.082 (11)	Na(1)–Na(2)	3.663 (9)

Table IV. Distances (Å) to the Mean Plane of Atoms Fe(1–9)

Fe(1)	−0.137	Fe(6)	−0.079	S(1)	1.055	S(9)	−0.460
Fe(2)	0.081	Fe(7)	0.086	S(2)	−1.430	S(10)	1.362
Fe(3)	0.028	Fe(8)	0.017	S(3)	1.551	S(11)	−1.648
Fe(4)	0.154	Fe(9)	−0.039	S(4)	−0.682	S(12)	0.980
Fe(5)	−0.113			S(5)	−1.647	S(13)	−0.648
		Na(1)	0.151	S(6)	0.839	S(14)	1.016
		Na(2)	2.658	S(7)	−0.864	S(15)	−1.625
				S(8)	1.322		

Cluster Structure. The compound $(n\text{-}Pr_4N)_6Na_4Fe_{18}S_{30}$·14MeCN crystallizes in space group $P\bar{1}$ with one-half anion, three $n\text{-}Pr_4N^+$, two Na^+, and seven MeCN solvate molecules in the asymmetric unit. The quaternary cations and acetonitrile molecules are well ordered and otherwise unexceptional and, as such, are not considered further. The structure of the cluster is shown in Figure 4, and a stereoview is provided in Figure 5. Metric

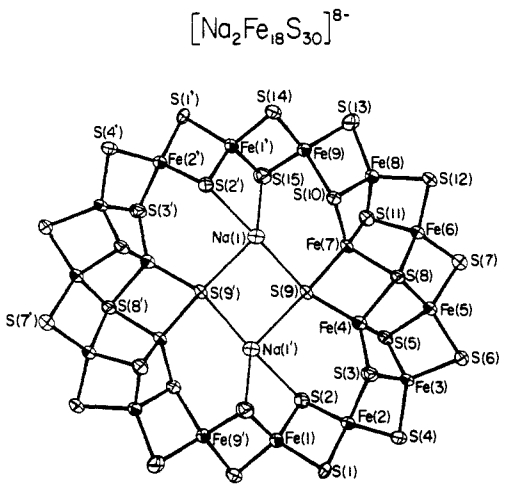

Figure 4. Structure of $[Na_2Fe_{18}S_{30}]^{8-}$ showing 50% probability ellipsoids and the atom-numbering scheme. Primed and unprimed atoms are related by an inversion center.

data are set out in Tables III–V.

Two remarkable features of the cluster are immediately apparent: it contains *no terminal ligands* and its Fe–S framework has a *cyclic* structure. Every FeS_4 unit is tetrahedral. The sulfide-rich interior provides a cavity that encapsulates two sodium ions, Na(1,1'), each of which is monosolvated. The cluster, therefore, is formulated as $[Na_2Fe_{18}S_{30}]^{8-}$. It has a disk-like or toroidal topology with dimensions of 13.32 × 15.98 Å and a thickness of 3.3 Å, which is twice the vertical displacement of S(5,11) from the Fe(1–18) mean plane (Table IV). The disks pack in the crystal with only translational symmetry, which results in parallel layers of anions, not unlike those found in many metal chalcogenide binary phases. In fact, the $Fe_{18}S_{30}$ portion of the anion can be envisioned as the prototype of an as yet unrealized layered Fe–S phase consisting of fused FeS_4 tetrahedra, to yield a material described as $^{2}_{\infty}[FeS_{4/x}]$ ($x > 2$). The Fe:S ratio of 0.6 is the lowest in any synthetic Fe–S cluster (Table I) and approaches the value of 0.5, which is found in a number of layered metal–chalcogenide phases.[25] Furthermore, the sulfide disposition throughout the cluster is not unlike a distorted hexagonal-close-packed *ab* bilayer.

The cluster has imposed centrosymmetry. Distortions owing to the presence of Na(1,1') interior to the cluster and Na(2,2') exterior to it reduce cluster symmetry from C_{2h} to the actual C_i. The latter two ions are more loosely associated with the cluster, at positions 2.66 Å above and below it, and are trisolvated. The $Fe_{18}S_{30}$ cycle is constructed, in the manner of Figure 1, by a combination of edge and vertex fusion of 24 Fe_2S_2 rhombs and is composed of three layers. With reference to Table IV, the central layer, which is the Fe_{18} plane, is perfect to within ±0.154 Å and includes the two encapsulated sodium ions Na(1,1'). Above and below this plane, at a distance of 0.68 Å is an uneven layer of sulfur atoms 0.97 Å thick. Between these layers reside central sulfur atoms S(9,9') at a distance of 0.460 Å from the Fe_{18} plane.

The edge-sharing and corner-sharing of Fe_2S_2 rhombs by which the $Fe_{18}S_{30}$ disk is conceptually generated encompass the fundamental modalities **2**, **3**, and **4** of Figure 1 and certain derivatives thereof. The cluster contains 20 μ_2-S + 8 μ_3-S + 2 μ_4-S; bridge multiplicities are assigned on the basis of interactions in the Fe–S framework. Iron vertex-sharing (**3**) results in the linear chain fragment Fe(1,2,9')-μ_2-S(1,2,14',15'), which resembles that found in $[Fe_3S_4(SR)_4]^{3-}$ (**14**). The most prevalent rhomb connectivity mode is edge-sharing (**2**), which occurs at Fe(3–5)S(3,5,6,8) and Fe(6–8)S(8,10–12) and generates two fragments **5**. Vertex juncture at μ_4-S(8) (**4**) and two further edge fusions achieved by addition of μ_2-S(7,9), as in transforming **4** into **11**, result in the fragment Fe(3–8)S(3,5–12). This corresponds to the Fe_6S_9 unit **13**, previously demonstrated in $[Fe_6S_9(SR)_2]^{4-}$ (**15**). Units **3** and **13** are connected by edge fusion at Fe(3)–S(3) and Fe(8)–S(10), and the pattern repeats around the ring.

With the recognition that $[Na_2Fe_{18}S_{30}]^{8-}$ consists of the fused substructures $2Fe_3S_4 + 2Fe_6S_9$, each of which has a single long dimension in discrete molecules, the question arises as to how a

Table V. Selected Angles (Deg) for $[Na_2Fe_{18}S_{30}]^{8-}$

Fe–Fe–Fe			
Fe(9')-Fe(1)-Fe(2)	164.00 (10)	Fe(7)-Fe(6)-Fe(5)	89.79 (8)
Fe(3)-Fe(2)-Fe(1)	157.53 (10)	Fe(8)-Fe(6)-Fe(5)	149.69 (9)
Fe(4)-Fe(3)-Fe(2)	83.05 (8)	Fe(8)-Fe(6)-Fe(7)	59.90 (7)
Fe(5)-Fe(3)-Fe(2)	144.55 (10)	Fe(6)-Fe(7)-Fe(4)	91.11 (8)
Fe(5)-Fe(3)-Fe(4)	61.70 (7)	Fe(8)-Fe(7)-Fe(4)	149.90 (10)
Fe(5)-Fe(4)-Fe(3)	58.74 (7)	Fe(8)-Fe(7)-Fe(6)	58.84 (7)
Fe(7)-Fe(4)-Fe(3)	147.38 (10)	Fe(7)-Fe(8)-Fe(6)	61.26 (7)
Fe(7)-Fe(4)-Fe(5)	88.65 (8)	Fe(9)-Fe(8)-Fe(6)	150.86 (9)
Fe(4)-Fe(5)-Fe(3)	59.56 (7)	Fe(9)-Fe(8)-Fe(7)	89.90 (8)
Fe(6)-Fe(5)-Fe(3)	149.92 (10)	Fe(8)-Fe(9)-Fe(1)	161.95 (10)
Fe(6)-Fe(5)-Fe(4)	90.37 (8)		
S–Fe–S			
(μ_2-S)–Fe–(μ_2-S)			
S(2)-Fe(1)-S(1)	102.88 (15)	S(4)-Fe(2)-S(2)	116.06 (18)
S(14)-Fe(1')-S(1')	117.55 (16)	S(6)-Fe(3)-S(4)	121.32 (16)
S(14)-Fe(1')-S(2')	109.70 (17)	S(7)-Fe(5)-S(6)	118.35 (16)
S(15)-Fe(1')-S(1')	110.99 (18)	S(12)-Fe(6)-S(7)	120.25 (16)
S(15)-Fe(1')-S(2')	112.38 (16)	S(13)-Fe(8)-S(12)	116.46 (17)
S(15)-Fe(1')-S(14)	103.62 (16)	S(14)-Fe(9)-S(13)	111.66 (17)
S(2)-Fe(2)-S(1)	105.08 (15)	S(15)-Fe(9)-S(13)	118.25 (21)
S(4)-Fe(2)-S(1)	114.45 (16)	S(15)-Fe(9)-S(14)	105.36 (17)
(μ_3-S)–Fe–(μ_3-S)			
S(3)-Fe(2)-S(1)	113.72 (17)	S(11)-Fe(6)-S(7)	114.81 (18)
S(3)-Fe(2)-S(2)	107.18 (15)	S(12)-Fe(6)-S(11)	102.38 (16)
S(4)-Fe(2)-S(3)	100.40 (15)	S(10)-Fe(7)-S(9)	119.29 (15)
S(4)-Fe(3)-S(3)	104.08 (16)	S(11)-Fe(7)-S(9)	116.07 (17)
S(5)-Fe(3)-S(3)	105.40 (15)	S(11)-Fe(7)-S(10)	104.33 (15)
S(5)-Fe(3)-S(4)	111.57 (17)	S(11)-Fe(8)-S(10)	103.88 (14)
S(6)-Fe(3)-S(3)	111.18 (17)	S(12)-Fe(8)-S(10)	113.42 (17)
S(6)-Fe(3)-S(5)	102.44 (15)	S(12)-Fe(8)-S(11)	103.82 (16)
S(5)-Fe(4)-S(3)	105.34 (15)	S(13)-Fe(8)-S(10)	105.03 (16)
S(9)-Fe(4)-S(3)	125.86 (16)	S(13)-Fe(8)-S(11)	113.75 (20)
S(9)-Fe(4)-S(5)	112.42 (17)	S(13)-Fe(9)-S(10)	100.95 (16)
S(6)-Fe(5)-S(5)	101.24 (15)	S(14)-Fe(9)-S(10)	113.29 (17)
S(7)-Fe(5)-S(5)	117.04 (17)	S(15)-Fe(9)-S(10)	107.49 (15)
(μ_4-S)–Fe–(μ_2-S)			
S(8)-Fe(4)-S(9)	103.38 (14)	S(8)-Fe(6)-S(7)	103.25 (15)
S(8)-Fe(5)-S(6)	113.74 (17)	S(8)-Fe(6)-S(12)	110.72 (17)
S(8)-Fe(5)-S(7)	102.36 (15)	S(8)-Fe(7)-S(9)	103.48 (14)
(μ_4-S)–Fe–(μ_3-S)			
S(8)-Fe(4)-S(3)	103.10 (15)	S(8)-Fe(6)-S(11)	104.58 (14)
S(8)-Fe(4)-S(5)	104.39 (14)	S(8)-Fe(7)-S(10)	107.24 (15)
S(8)-Fe(5)-S(5)	103.62 (14)	S(8)-Fe(7)-S(11)	105.37 (15)
Fe–S–Fe			
Fe–(μ_2-S)–Fe			
Fe(2)-S(1)-Fe(1)	75.46 (13)	Fe(7)-S(9)-Fe(4)	76.32 (13)
Fe(2)-S(2)-Fe(1)	74.41 (13)	Fe(8)-S(12)-Fe(6)	74.32 (13)
Fe(3)-S(4)-Fe(2)	75.14 (13)	Fe(9)-S(13)-Fe(8)	76.46 (14)
Fe(5)-S(6)-Fe(3)	74.86 (13)	Fe(9)-S(14)-Fe(1')	74.88 (14)
Fe(6)-S(7)-Fe(5)	77.50 (14)	Fe(9)-S(15)-Fe(1')	74.02 (14)
Fe–(μ_3-S)–Fe			
Fe(3)-S(3)-Fe(2)	71.52 (13)	Fe(8)-S(10)-Fe(7)	71.98 (13)
Fe(4)-S(3)-Fe(2)	101.94 (16)	Fe(9)-S(10)-Fe(7)	110.22 (17)
Fe(4)-S(3)-Fe(3)	72.97 (13)	Fe(9)-S(10)-Fe(8)	70.92 (12)
Fe(4)-S(5)-Fe(3)	72.73 (13)	Fe(7)-S(11)-Fe(6)	73.56 (13)
Fe(5)-S(5)-Fe(3)	71.76 (12)	Fe(8)-S(11)-Fe(6)	71.65 (13)
Fe(5)-S(5)-Fe(4)	74.07 (13)	Fe(8)-S(11)-Fe(7)	73.07 (13)
Fe–(μ_4-S)–Fe			
Fe(5)-S(8)-Fe(4)	72.28 (12)	Fe(7)-S(8)-Fe(4)	72.24 (12)
Fe(6)-S(8)-Fe(4)	113.63 (17)	Fe(7)-S(8)-Fe(5)	110.93 (17)
Fe(6)-S(8)-Fe(5)	71.79 (12)	Fe(7)-S(8)-Fe(6)	71.40 (12)

(25) (a) Hulliger, F. *Struct. Bonding (Berlin)* **1968**, *4*, 83. (b) Wells, A. F. *Structural Inorganic Chemistry*, 5th ed.; Clarendon Press: Oxford, 1984; Chapter 17.

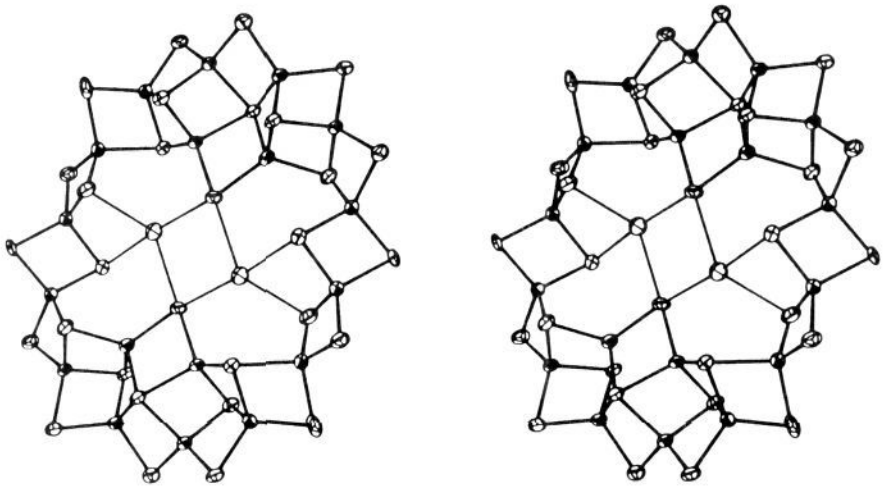

Figure 5. Stereoview of the structure of $[Na_2Fe_{18}S_{30}]^{8-}$.

ring is formed. Examination of Figure 1 shows that edge-sharing disposes Fe atoms in nonlinear arrangements such as in **5**, **9**, and **11**. This suggests that this type of rhomb fusion is utilized in "turning a corner". However, the Fe_{14} circumference of the ring is formed entirely by Fe vertex-sharing. In unperturbed extended vertex-sharing, Fe–Fe–Fe angles are expected to be 180°. In fact, these angles around the ring perimeter are all reduced from this value and range from 144.6° (Fe(5)–Fe(3)–Fe(2)) to 164.0° (Fe(9′)–(Fe(1)–Fe(2)). Two structural distortions could be implicated in this deviation from linearity: axial or other deformation of FeS_4 tetrahedra toward planarity, and nonplanarity of Fe_2S_2 rhombs. Limiting planar stereochemistry supports the formation of cyclic structures in the set $Ni_n(\mu_2\text{-}SR)_{2n}$ (n = 4, 6, 8).[26] Nonplanarity of rhombs is common in Fe–S clusters. While the FeS_4 tetrahedra are distorted, it is the nonplanar rhombs that are chiefly responsible for ring formation. Dihedral angles range from 11.1° for Fe(1′,9)S(14,15) to 23.8° for Fe(3,5)S(5,6). The largest distortions reside in the region of intersection of Fe_3S_4 and Fe_6S_9 subunits, while the smallest are with the former subunit.

The cluster is a mixed-valence species, having 14 Fe(III) and 4 Fe(II) or a mean Fe oxidation state of 2.78+. The usual ordering of mean Fe–S bond distances as dependent upon bridge multiplicity, i.e., Fe–μ_4-S (2.353 (9) Å) > Fe–μ_3-S (2.31 (3) Å) > Fe–μ_2-S (2.22 (2) Å), is observed. This order was first established with $[Fe_6S_9(SR)_2]^{4-}$.[13a] There is no clear structural evidence for localized oxidation states. Their recognition is difficult because of the different intrinsic Fe–S distances at constant oxidation state but variant bridge multiplicity. However, given the 0.14-Å difference in Fe(II) and Fe(III) Shannon radii[27] and the 0.10-Å difference observed in tetrahedral $[Fe(SR)_4]^{2-,1-}$ species,[28] sites of the type Fe(μ_2-S)(μ_3-S)$_2$(μ_4-S) would be the most hospitable to the Fe(II) state. They afford the least electron rich coordination environment and the longest mean bond distances, these being 2.30 Å at Fe(4) and 2.28 Å at Fe(7). On the other hand, the site Fe(1)(μ_2-S)$_4$ (2.25 Å) should be the most effective in localizing Fe(III), with the remaining sites presumably in between these extremes. Overall, metric features are unexceptional. The Na–S distances involving encapsulated Na(1,1′) are comparable to those in $[Na_2(Fe_6S_9(SMe)_2)_2]^{6-}$, where the sodium ions cause association of two Fe_6S_9 clusters by binding to μ_2-S and μ_4-S sites.[13b]

Tetrahedral Building Blocks. We recognize that, in addition to the scheme based on vertex- and edge-sharing of Fe_2S_2 rhombs laid out in Figure 1, a conceptual framework based on the fusion of FeS_4 tetrahedra can be utilized to construct all known Fe–S clusters as well as many Fe–chalcogenide phases. Outlined in

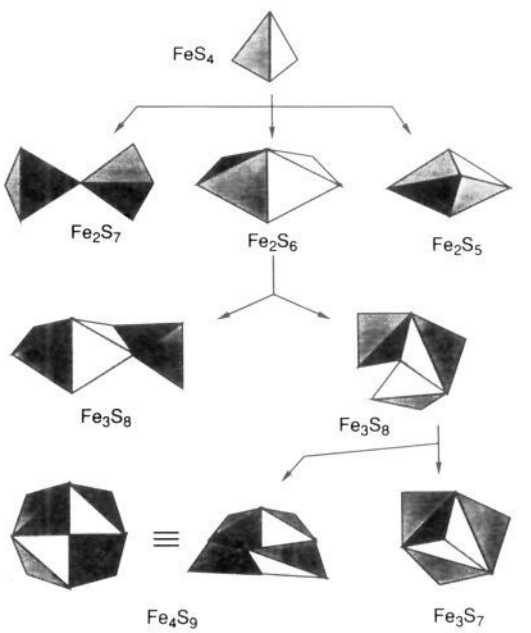

Figure 6. Schematic representation of the buildup of cluster units by connection of FeS_4 tetrahedra by vertex-sharing (Fe_2S_7), edge-sharing (Fe_2S_6), and face-sharing (Fe_2S_5). The remaining structures are developed by additional connectivity modes of these types.

Figure 6 are the three modes by which tetrahedra can be linked in a scheme parallel to that in Figure 1. The discrete FeS_4 unit has been realized in the phase Na_5FeS_4.[29] Vertex-sharing results in Fe_2S_7, as found in Ba_2FeS_3.[30] Edge-sharing gives Fe_2S_6, the sulfide-ligated form of Fe_2S_2, which is known in Na_3FeS_3.[31] Face-sharing affords Fe_2S_5, an as yet unknown fragment. Anti edge fusion of an additional tetrahedron to Fe_2S_6 gives linear Fe_3S_8, which is the prototype of the unidimensional polymers in M^IFeS_2[18] and $Na_3Fe_2S_4$[19] and is the sulfide-ligated version of cluster **14**. Syn edge fusion results in nonlinear Fe_3S_8, which can be closed to cyclic Fe_3S_7, found in $Ba_3Fe_3S_7$.[30] Further syn fusion results in Fe_4S_9, which is present in $Ba_8Fe_8S_{15}$[20a] and is contained in Fe_6S_{11}, the sulfide-ligated form of cluster **15** generated by the union of two Fe_3S_7 via common edges. As shown in Figure 7, the structure of $[Na_2Fe_{18}S_{30}]^{8-}$ is interpretable in terms of the connectivities of FeS_4 tetrahedra which afford Fe_3S_8 and Fe_6S_{11}.

(26) Dance, I. G.; Scudder, M. L.; Secomb, R. *Inorg. Chem.* **1985**, *24*, 1201.
(27) Shannon, R. D. *Acta Crystallogr., Sect. A* **1976**, *A32*, 751.
(28) Lane, R. W.; Ibers, J. A.; Frankel, R. B.; Papaefthymiou, G. C.; Holm, R. H. *J. Am. Chem. Soc.* **1977**, *99*, 84.
(29) Klepp, K. O.; Bronger, W. *Z. Anorg. Allg. Chem.* **1986**, *532*, 23.
(30) Hong, H. Y.; Steinfink, H. *J. Solid State Chem.* **1972**, *5*, 93.
(31) Müller, P.; Bronger, W. *Z. Naturforsch., B: Anorg. Chem., Org. Chem.* **1979**, *34B*, 1264.

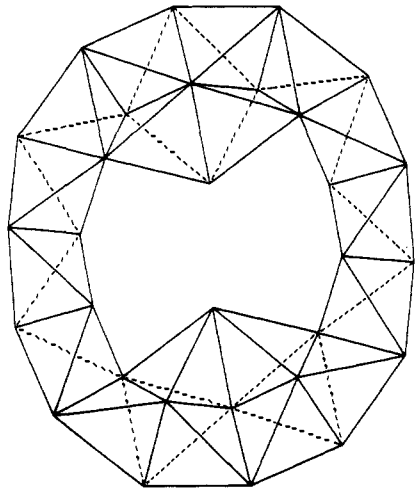

Figure 7. Conception of the structure of the $Fe_{18}S_{30}$ ring of $[Na_2Fe_{18}S_{30}]^{8-}$ in terms of FeS_4 tetrahedra connected by the modes of Figure 6.

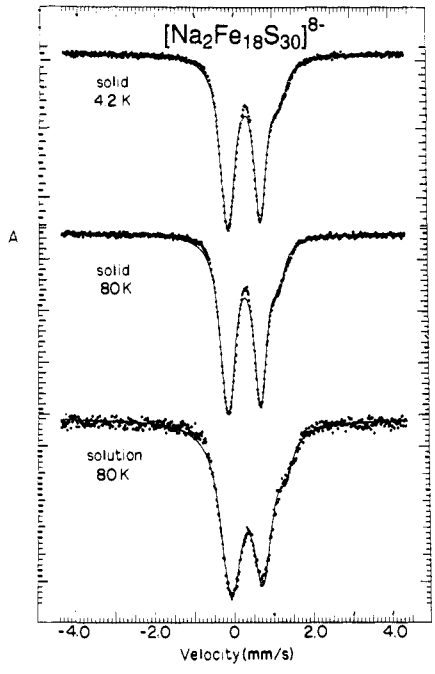

Figure 8. Mössbauer spectra of $(Pr_4N)_6Na_4Fe_{18}S_{30}$ at 4.2 and 80 K in the solid state and at 80 K in acetonitrile solution. The solid lines are theoretical fits of the spectra using the parameters of Table VI.

Thus the structure of this cluster, and the cores of the simpler clusters **14** and **15**, has been achieved, albeit via an alternative construct. Regardless of which construct is entertained, it is evident that, because of its size and structural relationship to Fe–S binary and ternary phases, $[Na_2Fe_{18}S_{30}]^{8-}$ lies at the boundary of molecular and solid-state compounds.

Electronic Properties. Physical measurements on the cylic cluster were made on its unsolvated compound, $(Pr_4N)_6Na_4Fe_{18}S_{30}$.

(a) Mössbauer Spectra. The ^{57}Fe Mössbauer spectra were examined in zero field at 1.6–180 K and under a longitudinally applied field of 80 kOe at 4.2 K. Zero-field spectra at two temperatures are shown in Figure 8 and consist of two apparent overlapping doublet features. The minority doublet appears as a shoulder of the positive-velocity side. No magnetic hyperfine structure is observed. Measurements of the chain compounds $NaFeS_2$, prepared at ambient temperature by the method of Taylor and Shoesmith,[24] and $(Et_4N)FeS_2$,[32] considered the most likely

(32) This compound was prepared by the procedure used for $(n\text{-}Pr_6N)_6Na_4Fe_{18}S_{30}$, except for the use of Et_4NCl in place of $n\text{-}Pr_4NBr$. Addition of the former to the reaction mixture afforded immediate precipitation of $(Et_4N)FeS_2$, which was collected and washed with ethanol and ether.

Table VI. Mössbauer Spectroscopic and Magnetic Properties of $(Pr_4N)_6Na_4Fe_{18}S_{30}$ and Chains and Related Clusters

Mössbauer Spectroscopic Properties

chain/cluster	T, K	δ,[a] mm/s	ΔE_Q, mm/s	Γ,[b] mm/s	% abs[c]	ref
$Na[FeS_2]$[d] (7)	80	0.19	0.56	0.42		e
$Et_4N[FeS_2]$[d] (7)	80	0.18	0.71	0.41		e
	200	0.11	0.64	0.41		
$[Fe_3S_4(SEt)_4]^{3-}$ (**14**)	77	0.12	0.52	0.60		36
$[Fe_3S_4(SPh)_4]^{3-}$ (**14**)	77	0.17	0.63	0.68		36
$[Fe_6S_9(S\text{-}t\text{-}Bu)_2]^{4-}$ (**15**)	4.2	0.29	0.72	*f*	*f*	37
		0.28	0.43	*f*	*f*	37
$[Na_2Fe_{18}S_{30}]^{8-}$, solid	4.2	0.18	0.81	0.37	83	e
		0.34	1.49	0.37	17	
	80	0.16	0.81	0.39	85	
		0.32	1.46	0.32	15	
	180	0.12	0.99	0.38	86	
		0.27	1.42	0.27	14	
$[Na_2Fe_{18}S_{30}]^{8-}$, MeCN soln	4.2	0.21	0.79	0.54	84	e
		0.41	1.67	0.44	16	
	80	0.21	0.77	0.60	89	
		0.41	1.59	0.36	11	
	180	0.16	0.73	0.60	88	
		0.32	1.47	0.40	12	

Magnetic Properties

cluster	μ_{eff},[g] μ_B (T, K)	ref
$[Na_2Fe_{18}S_{30}]^{8-}$, solid	0.31 (15.0), 0.91 (27.0), 1.93 (55.0), 2.53 (80.1), 2.93 (100.0), 3.79 (150.2), 4.24 (170.1), 4.65 (179.7), 5.45 (267.7), 5.96 (304.2)	e

[a] Relative to Fe metal at 4.2 K. [b] Line width. [c] Percent of total absorption. [d] Prepared by low-temperature methods.[24,32] [e] This work. [f] Not reported. [g] Magnetic susceptibilities measured at 5 kOe.

impurities, established that these compounds are not responsible for the shoulder feature. They and other M^1FeS_2 compounds at 4.2 K show six-line magnetic hyperfine spectra whose isomer shifts (δ) and quadrupole splittings (ΔE_Q) are cation dependent.[33-35]

The spectrum in a longitudinally applied 80-kOe field at 4.2 K consists of a four-line pattern arising from the $\Delta M_I = \pm 1$ transitions of the majority Fe site with the magnetic field at the nucleus equal to the applied field. This observation is consistent with a singlet ground state.

The cluster contains nine crystallographically distinct Fe sites. As would be expected, subspectra of these sites, all of which are of the tetrahedral FeS_4 type, are unresolved. Attempts to fit the spectra with a three-site model, with and without certain parameter constraints, did not converge to a unique result. Spectral fits based on a two-site model with no parameter constraints are shown in Figure 8. The spectral parameters are given in Table VI together with data for clusters **14** and **15**.[36,37] With this model, the intensity ratio of the two doublets is 4.9:1 at 4.2 K. As calculated from the empirical relationship between isomer shift and oxidation state for tetrahedral FeS_4 sites,[38] the majority doublet corresponds to an oxidation state of 2.93+ and the minority doublet to 2.55+. The weighted average of these is 2.87+, which agrees well with mean oxidation state of 2.78+ from the chemical formula. Under the two-site model, the majority quadrupole doublet corresponds to sites that approach the ferric state, as may be further seen by comparison of the isomer shift with that for **14**. No individual ferrous sites, for which $\delta = 0.5$–0.7 mm/s and $\Delta E_Q \approx 3$ mm/s,[28,39]

(33) Raj, D.; Puri, K. P. *J. Chem. Phys.* **1969**, *50*, 3184.
(34) Taft, C. A. *J. Phys. (Les Ulis, Fr.)* **1977**, *38*, 1161.
(35) Cooper, D. M.; Dickson, D. P. E.; Domingues, P. H.; Gupta, G. P.; Johnson, C. E.; Taft, C. A.; Walker, P. J. *J. Magn. Magn. Mater.* **1983**, *36*, 171.
(36) Girerd, J.-J.; Papaefthymiou, G. C.; Watson, A. D.; Gamp, E.; Hagen, K. S.; Edelstein, N.; Frankel, R. B.; Holm, R. H. *J. Am. Chem. Soc.* **1984**, *106*, 5941.
(37) Christou, G.; Holm, R. H.; Sabat, M.; Ibers, J. A. *J. Am. Chem. Soc.* **1981**, *103*, 6269.
(38) Christou, G.; Mascharak, P. K.; Armstrong, W. H.; Papaefthymiou, G. C.; Frankel, R. B.; Holm, R. H. *J. Am. Chem. Soc.* **1982**, *104*, 2820.

were indicated by the treatment. We conclude that, in this respect, the cluster is delocalized, as is the case for **15** and all other mixed-valence Fe–S clusters in Table I.

(b) Magnetism. Magnetization and magnetic susceptibility properties were examined at 1.8–310 K. The data for all preparations indicated the presence of a paramagnetic impurity, for which a correction was made by fitting the observed susceptibility at $T \leq 10$ K to the Curie–Weiss law. The corrected susceptibilities for different preparations were reproducible to within 2–4% over the entire temperature range. Magnetic moments are entered in Table VI. The χ^M vs T behavior (not shown) is indicative of an antiferromagnetic species with a singlet ground state. The latter is consistent with the Mössbauer results. The magnetic moment per Fe atom at 304 K, $\mu_{Fe} = 1.40\ \mu_B$, is closely comparable with the ambient temperature μ_{Fe} values for clusters of the types $[Fe_2S_2(SR)_4]^{2-}$ (1.4 μ_B),[40] $[Fe_4S_4(SR)_4]^{2-}$ (1.1 μ_B),[41] and $[Fe_6S_9(SR)_2]^{4-}$ (1.1–1.2 μ_B).[13a,b] $[Na_2Fe_{18}S_{30}]^{8-}$ joins the set of even-electron Fe–S clusters (Table I), all of which are antiferromagnetically coupled with a singlet ground state. Because of the complexity of the spin system, we have not attempted to evaluate a coupling constant J from the magnetic data.

Solution Structure. The absence of terminal organic ligands in $[Na_2Fe_{18}S_{30}]^{8-}$ eliminates ^1H and ^{13}C NMR methods for investigation of solution structure. This property has been examined by absorption spectra, ^{23}Na NMR, and Mössbauer spectroscopy.

(a) Absorption Spectra. The UV/visible spectrum in Figure 3 reveals only shoulders in the visible region and two resolved maxima in the near-UV region. Note that because of the presence of Fe_3S_4 and Fe_6S_9 substructures, spectra[5] of $[Fe_3S_4(SEt)_4]^{3-}$ and $[Fe_6S_9(SEt)_2]^{4-}$ are included in Figure 3 together with a calculated spectrum that is twice the sum of these spectra. There is a rough correspondence between the calculated spectrum and that of the cyclic cluster, viz., strong bands near 300 and 400 nm and weaker shoulders in the 500–600-nm region. A close correspondence is not expected because of the likely interactions between substructure chromophores and the contribution of $EtS^- \rightarrow$ core charge-transfer bands to the spectra.

(b) ^{23}Na NMR. Spectra of ca. 10 mM solutions of $(Pr_4N)_6Na_4Fe_{18}S_{30}$ in acetonitrile are complicated by exchange processes involving the two types of sodium ions in the structure and NaCl impurity. At 230 K, the slow-exchange limit is approached and the spectrum consists of signals at 19 and 375 ppm, with the former more intense. When 2 equiv of 18-crown-6 was added and the solution examined at 297 K, the system appeared to be at or near slow exchange, and resonances were observed at 15 and 470 ppm. The more intense, upfield signal arises from the Na^+/crown ether complex and any free Na^+ present, leaving the downfield resonance assignable to Na^+ contained in the cyclic cluster. Very similar results were obtained with 10 equiv of the crown ether. We conclude that in solution the cluster retains its two interior sodium ions.

(c) Mössbauer Spectrum. A spectrum of the cluster at 80 K in acetonitrile solution, together with a two-site spectral fit using the parameters in Table VI, is included in Figure 8. Other than broader lines, solution spectra are quite comparable to solid-state spectra at the same temperature.

We conclude that the cyclic cluster structure and the sequestered sodium ions are retained in solution. Further, there is no indication from either absorption spectra (Figure 2) or Mössbauer spectroscopy of the presence of a detectable quantity of the most likely impurity, the chain polymer **7**. In the sense of retaining the interior sodium ions, cyclic cluster $[Fe_{18}S_{30}]^{10-}$ is itself an "inorganic crown thioether".

Reactivity. (a) With Thiol. One prospect presented by the structure of $[Na_2Fe_{18}S_{30}]^{8-}$ is its cleavage into smaller cluster fragments, which may not have been previously prepared. Thiol or thiolate is the initial reagent of choice for this purpose inasmuch as thiolate functions as a stabilizing terminal ligand in the great majority of clusters in Table I. Treatment of the cluster in acetonitrile solution with 1, 2, 4, 8, 18, and 36 equiv of *p*-toluenethiol for ca. 1 h at ambient temperature gave dark brown solutions. The only isotropically shifted resonances of appreciable intensity in the ^1H NMR spectra of these solutions are those of $[Fe_4S_4(S\text{-}p\text{-}tol)_4]^{2-}$ (5.19 (*p*-H), 5.71 (*o*-H), 8.17 (*m*-H) ppm).[42] Spectra measured 1–4 days later showed intensified cluster signals. After the solutions were heated at 65 °C for 1.5 h and cluster signals were integrated vs Pr_4N^+ resonances, conversion to the cluster was ca. 100% based on thiol added.

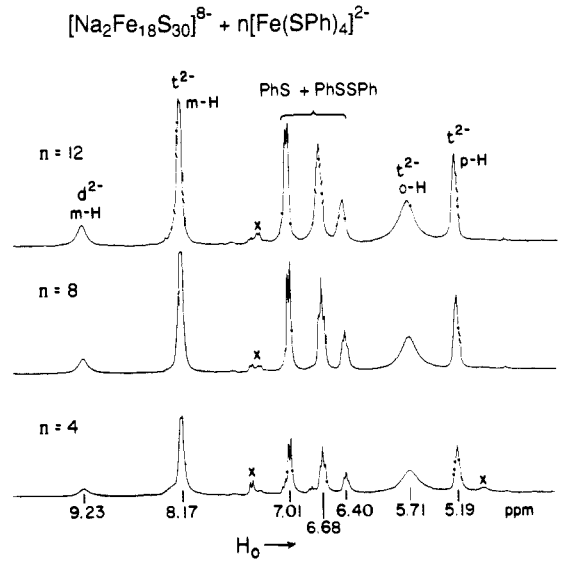

Figure 9. ^1H NMR spectra of solutions resulting from the reactions of 1.7–2.5 mM $(Pr_4N)_6Na_4Fe_{18}S_{30}$ with 4–12 equiv of $(Et_4N)_2[Fe(SPh)_4]$ in Me_2SO-d_6 at ca. 25 °C. Each spectrum corresponds to a separate reaction system measured 2 days after mixing. Signal assignments refer to $[Fe_4S_4(SPh)_4]^{2-}$ (t^{2-}) or $[Fe_2S_2(SPh)_4]^{2-}$ (d^{2-}); × = probable diamagnetic species.

(b) With Thiolate and $[Fe(SPh)_4]^{2-}$. No reaction was observed between $[Na_2Fe_{18}S_{30}]^{8-}$ and up to 36 equiv of NaSPh and Pr_4N-(SPh) in Me_2SO and acetonitrile solutions, respectively, for 1 h at 60 °C. However, systems containing 2, 4, 8, 12, 16, and 32 equiv of $(Et_4N)_2[Fe(SPh)_4]$ in Me_2SO solutions reacted at room temperature to afford $[Fe_4S_4(SPh)_4]^{2-}$ as the principal product. The ^1H NMR spectra of several reaction systems are shown in Figure 9, where the formation of the tetranuclear cluster with its characteristic resonances[42] is clearly evident. Yields in situ of 44–52% based on Fe were obtained from signal intensities. Very similar yields were evaluated from the absorption band of $[Fe_4S_4(SPh)_4]^{2-}$ at 460 nm. The isotropically shifted signal at 9.23 ppm is assigned to $[Fe_2S_2(SPh)_4]^{2-}$.[43] In the experiments in Figure 9, the mole ratio $[Fe_4S_4(SPh)_4]^{2-}$:$[Fe_2S_2(SPh)_4]^{2-}$ varied from 5.7:1 at $n = 4$ to 3:1 at $n = 12$.

From the foregoing results, it is apparent that reactions of $[Na_2Fe_{18}S_{30}]^{8-}$ with the electrophilic reagents *p*-toluenethiol and $[Fe(SPh)_4]^{2-}$ effect rupture of the cyclic framework. However, the majority or exclusive products of these reactions are the well-known clusters $[Fe_4S_4(SR)_4]^{2-}$, with $[Fe_2S_2(SPh)_4]^{2-}$ a detectable minority product in reactions with $[Fe(SPh)_4]^{2-}$.[44] In this sense, the cyclic cluster resembles $[Fe_6S_9(S\text{-}t\text{-}Bu)_2]^{4-}$, which affords the corresponding cubane-type cluster upon reaction with

(39) Coucouvanis, D.; Swenson, D.; Baenziger, N. C.; Murphy, C.; Holah, D. G.; Sfarnas, N.; Simopoulos, A.; Kostikas, A. *J. Am. Chem. Soc.* **1981**, *103*, 3350.

(40) Gillum, W. O.; Frankel, R. B.; Foner, S.; Holm, R. H. *Inorg. Chem.* **1976**, *15*, 1095.

(41) Laskowski, E. J.; Frankel, R. B.; Gillum, W. O.; Papaefthymiou, G. C.; Renaud, J.; Ibers, J. A.; Holm, R. H. *J. Am. Chem. Soc.* **1978**, *100*, 5322.

(42) Reynolds, J. G.; Laskowski, E. J.; Holm, R. H. *J. Am. Chem. Soc.* **1978**, *100*, 5315.

(43) Reynolds, J. G.; Holm, R. H. *Inorg. Chem.* **1980**, *19*, 3257. In this reference the shifts of $[Fe_2S_2(SPh)_4]^{2-}$ were reported in acetonitrile solution. In Me_2SO, the solvent used here, the shifts differ only slightly (δ 9.27 (*m*-H), 4.9 (br, *o*-H), 3.45 (*p*-H)).

(44) In reactions with *p*-toluenethiol, a slight extent of formation of $[Fe_2S_2(S\text{-}p\text{-}tol)_4]^{2-}$ is indicated by the appearance of a broad signal near 9.2 ppm.[43]

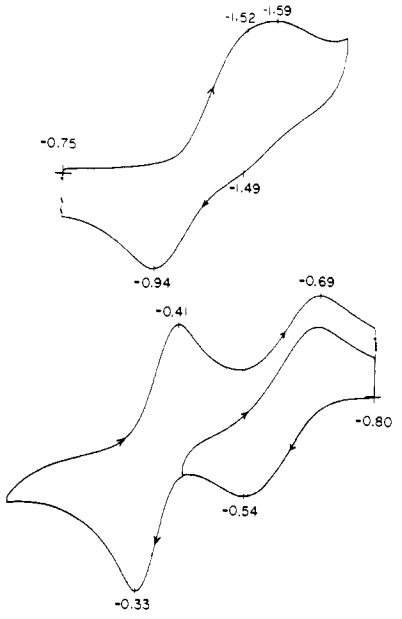

Figure 10. Cyclic voltammograms of $[Na_2Fe_{18}S_{30}]^{8-}$ in DMF solution (100 mV/s) with scans to less negative (left) and more negative (right) potentials from the rest potential.

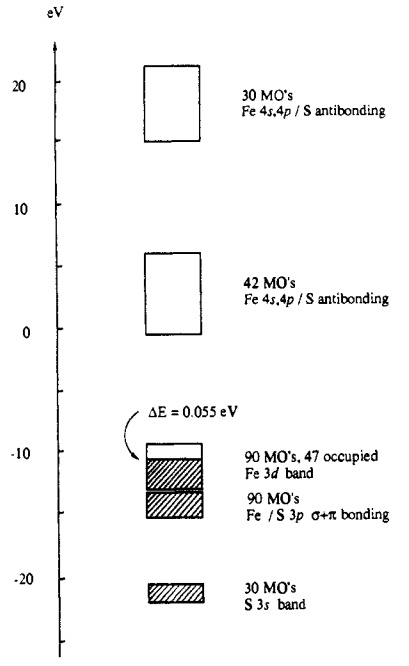

Figure 11. Block representation of the MO energy level diagram of $[Fe_{18}S_{30}]^{10-}$ as calculated by the extended-Hückel method. The dominant orbital components of each block are indicated; occupied blocks or bands are shaded.

excess PhSH.[13a] The clusters $[Fe_4S_4(SR)_4]^{2-}$ once again emerge as the thermodynamically favored product in a system containing Fe(II,III), a sulfide source, and thiolate.

(c) Redox. The cyclic voltammograms (Figure 10) reveal that $[Na_2Fe_{18}S_{30}]^{8-}$ supports two oxidations: a quasi-reversible step with $E_{1/2} = -0.62$ V and a chemically reversible step with $E_{1/2} = -0.37$ V. These steps are followed at less negative potentials by multielectron oxidation, a feature common to many Fe–S clusters. The two steps are almost certainly one-electron processes; however, attempts to verify this by coulometry were unsuccessful because of the instability of the oxidized species. One or perhaps two irreversible reductions occur at −1.5 to −1.6 V. Given that $[Fe_6S_9(SR)_2]^{4-}$ clusters (R = Ph, Et, *t*-Bu) undergo reversible one-electron oxidations at −0.50 to −0.63 V,[5,13a] it is possible that the sites of oxidation are the Fe_6S_9 substructures. These clusters and $[Fe_3S_4(SR)_4]^{3-}$[5] undergo reductions at comparably negative potentials (<−1.4 V, R constant).

Molecular Orbital Description. Lastly, an approximate MO description of the cyclic cluster has been sought. Given the size and complexity of the molecule, calculations were performed at the extended-Hückel level[45,46] on $[Na_2Fe_{18}S_{30}]^{8-}$ and $[Fe_{18}S_{30}]^{10-}$ with crystallographic C_i symmetry. Related calculations by Silvestre and Hoffmann[46] have provided useful insights into the electronic structures of M^IFeS_2 chain compounds. Results for $[Fe_{18}S_{30}]^{10-}$ are presented in the form of the energy level diagram in Figure 11. The 282 MOs are packed in four or five blocks or "bands" whose principal orbital components are indicated. In the lowest block the most stable 30 orbitals are essentially nonbonding S 3s orbitals. This implicates the 3p orbitals as those mainly involved in bonding to the Fe atoms, consistent with the results of corresponding calculations on other Fe–S clusters.[47]

The next region consists of two groups of 90 MOs each whose separation is strongly dependent on the 3d H_{ii} Fe parameter. The scheme depicted was obtained by using the same H_{ii} value as employed in calculations of Fe–S chains and clusters by Hoffmann and co-workers.[46-48] The orbitals of the lower group are densely packed in a 3.9-eV interval, have Fe 3d, 4s, and 4p and S 3p character, and are mainly responsible for the Fe–S bonding interactions. The next group of 90 MOs is spread over an interval of 6.5 eV with 47 orbitals occupied, in accord with the singlet ground state. These orbitals have appreciable Fe character, account for Fe–Fe bonding and Fe–S antibonding interactions, and may be further described as follows. Eighteen correspond mainly to Fe–S π-antibonding, roughly canceling the effects of 18 such orbitals in the 90-orbital Fe–S bonding group. This reduces to 72 the number of effective Fe–S interactions, which is 4 times the number of μ_4-S atoms, 3 times the number of μ_3-S atoms, and 2 times the number of μ_2-S atoms, i.e., the number of Fe–S connections in the cluster. Of the remaining 29 filled orbitals in the block, 24 are mainly Fe–Fe bonding (equal to the number of Fe–Fe bonding connections) and 5 are essentially nonbonding. The apparent HOMO–LUMO separation is 0.055 eV.

The following principal conclusions are drawn from the calculations. (1) The cluster has a quasi-band structure in which orbitals divide into at least four well-separated blocks. (2) On the basis of overlap population differences on addition or removal of a pair of electrons, the HOMO and LUMO are weakly Fe–S and Fe–Fe antibonding. Filled orbitals are extensively delocalized. (3) The small HOMO–LUMO gap is consistent with the thermal population of paramagnetic states, as observed in the magnetism. (4) The average of the net charges of atoms Fe(4,4′) and Fe(7,7′) is 20% less than that of the remaining Fe atoms, suggesting, as from structural considerations, that these are the four quasi-ferrous atoms whose presence is reflected by the isomer shifts in Table VI. (5) The net charges at the sulfur atoms decrease with increasing bridge multiplicity, and the overlap populations follow the order Fe–μ_2-S > Fe–μ_3-S > Fe–μ_4-S, consistent with Fe–S bond distances. (6) Inclusion of two Na^+ ions in the calculation has no effect on the general energy level scheme, stabilizes Fe/S- and Fe-type orbitals, and causes lowered charges on bonded sulfur atoms.

The results of the calculations, while imprecise, serve to underscore the unique nature of $[Na_2Fe_{18}S_{30}]^{8-}$, which as a cyclic cluster has no precedent among known molecular species. The "bandlike" MO structure of the $Fe_{18}S_{30}$ ring, as opposed to a spread of discrete orbitals, raises the possibility of extended solid-state behavior not unlike that of the chains in M^IFeS_2.[46] Certain of these compounds show long-range magnetic order at 4.2 K. Similar behavior is not found in the magnetic behavior

(45) Na parameters: Burdett, J. K. *Molecular Shapes*; Wiley: New York, 1980; Chapter 2.
(46) Fe and S parameters: Silvestre, J.; Hoffmann, R. *Inorg. Chem.* **1985**, *24*, 4108.
(47) Sung, S.-S.; Glidewell, C.; Butler, A. R.; Hoffmann, R. *Inorg. Chem.* **1985**, *24*, 3856.
(48) Reduction of 3d H_{ii} by 9% (to give a parameter value used in other calculations[49]) causes the separation of the two groups to increase from 0.5 eV (as shown) to 2.6 eV.
(49) Tatsumi, K.; Hoffmann, R. *J. Am. Chem. Soc.* **1981**, *103*, 3328.

of $[Na_2Fe_{18}S_{30}]^{8-}$ (absence of magnetic hyperfine interactions in its Mössbauer spectra), owing to the large separation between rings. This preserves the low magnetic dimensionality nature of the ring, and no long-range magnetic order is expected above absolute zero.[50] For $N \geq 10$ interacting spins $S = {}^1/_2$ in a linear chain (such as are present in some M^1FeS_2 phases), theory predicts that low magnetic dimensionality solid-state effects become evident in magnetic properties.[51,52] Linear magnetic structures such as M^1FeS_2 do not undergo long-range order magnetic phase transitions until the interchain interaction becomes significant enough to drive the system into a three-dimensional magnetic order.[53]

The existence and stability of $[Na_2Fe_{18}S_{30}]^{8-}$ raise a number of questions for further investigation. These include the existence of other cyclic Fe/S structures, removal of the interior Na^+ ions and the stability of $[Fe_{18}S_{30}]^{10-}$, the ability to bind cations other than Na^+ in the cluster interior, and the existence of an analogous (or some other) Fe/Se cluster in which the interior void would be larger and the affinity for Na^+ presumably less.

Acknowledgment. This research was supported by NIH Grant 28856 at Harvard University and by the National Science Foundation at M.I.T. X-ray diffraction equipment was obtained through NIH Grant 1 S10 RR 02247. G.C.P. acknowledges support by the Office of Naval Research program on Cluster Science and Dynamics under Contract No. N00014-89-J-1779. We thank Dr. J. Gao for assistance with the MO calculations.

Supplementary Material Available: Crystallographic data for $(Pr_4N)_6Na_4Fe_{18}S_{30}\cdot 14MeCN$ including tables of data collection parameters, atomic coordinates, thermal parameters, and calculated hydrogen atom positions (7 pages); a table of calculated and observed structure factors (48 pages). Ordering information is given on any current masthead page.

(50) de Jongh, L. J.; Miedema, A. R. *Adv. Phys.* **1974**, *23*, 1.
(51) Bonner, J. C.; Fisher, M. E. *Phys. Rev.* **1964**, *135*, 4640.
(52) des Cloizeaux, J.; Pearson, J. J. *Phys. Rev.* **1962**, *128*, 2131.
(53) Carlin, R. L. *Magnetochemistry*; Springer-Verlag: New York, 1986.

Structural, Spectroscopic, and Chiroptical Properties of the Chiral Quadruple-Bonded Dimolybdenum Complexes $Mo_2Cl_4[(R,R)\text{-DIOP}]_2$ and $Mo_2Cl_4[(S,S)\text{-DIOP}]_2$

Jhy-Der Chen, F. Albert Cotton,* and Larry R. Falvello

Contribution from the Department of Chemistry and Laboratory for Molecular Structure and Bonding, Texas A&M University, College Station, Texas 77843. *Received July 10, 1989*

Abstract: By reaction of $K_4Mo_2Cl_8$ with (*R,R*)- or (*S,S*)-DIOP, (-)- or (+)-2,3-*O*-isopropylidene-2,3-dihydroxy-1,4-bis(diphenylphosphino)butane, two complexes of $Mo_2Cl_4(DIOP)_2$ were prepared. Their UV-vis, CD, and NMR spectra have been recorded, and the crystal structure of $Mo_2Cl_4[(R,R)\text{-DIOP}]_2$ has been determined. Crystal data: space group $P\bar{1}$, a = 13.406 (8) Å, b = 13.187 (3) Å, c = 11.855 (4) Å, α = 116.34 (2)°, β = 109.69 (3)°, γ = 100.70 (3)°, V = 1623 (3) Å^3, Z = 1. Final residuals: R = 0.0525 and R_w = 0.0728. The structure is disordered so that while only one set of ligand atoms can be resolved, there are two incompletely occupied sets of metal atom positions. In effect there are two different molecules, which have opposite chiralities about the Mo–Mo axis but very similar packing requirements, that randomly occupy the crystal sites. The primary form (P), which is Λ-$Mo_2Cl_4[(R,R)\text{-DIOP}]_2$, occupies 89% of the sites, while the Δ molecules (S) occupy the remaining 11%. The P molecules have a twist angle of −78° and the S molecules an angle of 87°. The ^{1}H NMR spectrum of a solution in CH_2Cl_2 shows that both molecules are again present but now in a P/S ratio of 1.7. Assignment of the various signals to the P and S molecules was possible on an a priori basis because the large diamagnetic anisotropy of the Mo–Mo quadruple bond affects corresponding hydrogen atoms in the two molecules in predictably different ways. An anisotropy of $(5700 \pm 1200) \times 10^{-36}$ m^3 molecule^{-1} is estimated. The CD spectra of both the *R,R* and *S,S* complexes are found to be fully in accord with the theoretical prediction that a Λ molecule with a twist angle $90° - \chi$ will have the same signs for the CD bands as a Δ molecule with a twist angle χ. The correct absolute sign is predicted in all cases. The UV-vis spectrum is in accord with the twist angle.

Dinuclear, metal–metal-bonded complexes of stoichiometry $M_2X_4(LL)_2$, where LL is a bidentate ligand such as $R_2PCH_2CH_2PR_2$, were first shown by Walton and co-workers[1] to be capable of existing in two isomeric forms, α and β, shown schematically in Figure 1 as a and b. It was soon recognized that the actual structure of the β isomers entails a twist about the metal–metal bond, and many of the electronic, spectroscopic, and structural consequences of this have been investigated in detail.[2,3] One of the most important consequences of the internal twist is that β-$M_2X_4(LL)_2$ molecules are chiral, and this particular phenomenon has been the subject of several previous studies.[4,5] In these investigations it has been shown that there is a simple and rigorous relationship between the direction and magnitude of the internal helicity and the sign of the CD band for the $\delta \rightarrow \delta^*$ transition in those molecules where such a transition is observed.

Another interesting aspect of β-$M_2X_4(LL)_2$ compounds is that generally, though not always, they form crystals in which two conformers that are different (and, importantly, of opposite helicity[6]) occupy each crystallographic site, albeit to different extents.[7] It turns out that these pairs of molecules have very similar arrangements of the ligand atoms in space even though, within a framework approximating to both, the M_2 unit takes one of two different and mutually orthogonal directions. It is the gross outward similarity of the two ligand arrangements that permits the disordered packing of the two types of molecule in the same crystal. However, since the two molecules are merely similar but not identical, even as seen from the outside by their neighbors, they are present in different amounts, one being the P (principal

(1) Ebner, J. R.; Tyler, D. R.; Walton, R. A. *Inorg. Chem.* **1976**, *15*, 833.
(2) Campbell, F. L., III; Cotton, F. A.; Powell, G. L. *Inorg. Chem.* **1985**, *24*, 177.
(3) Campbell, F. L., III; Cotton, F. A.; Powell, G. L. *Inorg. Chem.* **1985**, *24*, 4384.
(4) Agaskar, P. A.; Cotton, F. A.; Fraser, I. F.; Manojlovic-Muir, L.; Muir, K. W.; Peacock, R. D. *Inorg. Chem.* **1986**, *25*, 2511.
(5) Peacock, R. D. *Polyhedron* **1987**, *6*, 715.
(6) Agaskar, P. A.; Cotton, F. A. *Inorg. Chem.* **1984**, *23*, 3383.
(7) Brencic, J. V.; Cotton, F. A. *Inorg. Chem.* **1970**, *9*, 351.

0002-7863/90/1512-1076$02.50/0